Improved Thermal Stability and Mechanical Properties of Poly(propylene carbonate) by Reactive Blending with Maleic Anhydride

Meijun Yao, Fang Mai, Hua Deng, Nanying Ning, Ke Wang, Qiang Fu

College of Polymer Science and Engineering, State Key Laboratory of Polymer Materials Engineering, Sichuan University, Chengdu 610065, China

Received 4 March 2010; accepted 3 October 2010
DOI 10.1002/app.33565
Published online 14 February 2011 in Wiley Online Library (wileyonlinelibrary.com).

ABSTRACT: To extend the application of a carbon dioxide sourced environmental friendly polymer: poly (propylene carbonate) (PPC), a small amount of maleic anhydride (MA) was melt blended to end-cap with PPC to improve its thermal stability and mechanical properties. Thermal and mechanical properties of end-capped PPC were investigated by TGA, GPC, mechanical test, and DMA. TGA and titration results demonstrate that PPC can be easily end-capped with MA through simple melt blending. TGA results show that the thermal degradation temperature of PPC could be improved by around 140°C by adding MA. GPC measurement indicates that the molecular weight of PPC can be maintained after blending with MA, where pure PPC experiences a dramatic degradation in molecular weight during melt process. More importantly, the tensile strength of PPC after blending with MA was found to be nearly eight times higher than that of pure PPC. It has approached the mechanical properties of polyolefin polymers, indicating the possibility of replacing polyolefin polymers with PPC for low temperature applications. The method described here could be used to extend the applications of PPC and fight against the well known global warming problem. © 2011 Wiley Periodicals, Inc. J Appl Polym Sci 120: 3565–3573, 2011

Key words: poly (propylene carbonate); maleic anhydride; end-capping; thermal degradation; mechanical properties

INTRODUCTION

It is well known that the pollution derived from packaging materials has become a worldwide environmental problem. Recently, many efforts[1–4] have been made to develop new biodegradable materials to replace the conventional nondegradable or incompletely degrading synthetic polymers (e.g., polyolefin) to solve this challenging problem. Many renewable resource-based biopolymers such as bacterial polyesters,[5] and soy-based plastics[6,7] have been investigated. Besides, a new thermoplastic polymer Poly (propylene carbonate) (PPC) also shows biodegradability and has recently attracted much attention from many scientists.

PPC is derived from carbon dioxide and propyleneoxide.[8] Therefore, widely replacing other polymers with PPC can be used as an effective method to reduce carbon dioxide content in the atmosphere, to help solve the widely known global warming problem. Furthermore, PPC has interesting physical and chemical properties as well. It can be used as adhesives, solid electrolytes, polyols, photoresists, propellants, barrier materials, flexibilizers, and plasticizers.[9] Nevertheless, the flexible carbonate groups in their backbone chains have created many problems, including noncrystallinity, poor processing stability, poor mechanical properties, and poor thermal stability, which limited the applications of PPC. Therefore, many efforts have been devoted to improving the mechanical, thermal and other properties of PPC.[10–21] Xu et al.[5] have successfully prepared intercalation-exfoliation PPC/clay nanocomposites by direct melt intercalation in an internal mixer. They found that the thermal decomposition temperature of the nanocomposites was obviously improved with increasing clay content due to the shielding effect of clays. The storage modulus and Young's modulus of the nanocomposites could be very much improved comparing with neat PPC. The high loading level of fillers leads to the deteriorative properties, such as the increase in density and the loss of tenacity due to the interfacial incompatibility between PPC and the filler. Furthermore, Ma et al.[6] prepared the blends of poly (lactic acid) (PLA) and PPC at different ratios, they reported that the thermal stability of PPC could be improved by blending with PLA. However, the thermal stability of the blends is still lower than that of neat PLA. The

Correspondence to: H. Deng (huadeng@scu.edu.cn) or Q. Fu (qiangfu@scu.edu.cn).

Contract grant sponsor: National Natural Science Foundation of China; contract grant numbers: 20874064, 50873063, 50973065.

mechanism might be that the degradation products of PPC would facilitate the thermal degradation of PLA. To improve the thermal and mechanical performances of PPC, other biodegradable polymers, such as poly(ε-caprolactone) or poly (3-hydroxybutyrate) were also blended with PPC,[7,9] but not much improvement has been reported. Tao et al.[22] prepared UV-crosslinkable PPC by the terpolymerization of CO_2, propylene oxide (PO), and allyl glycidyl ether (AGE). The crosslinked PPC showed obvious improvement in thermal and mechanical properties in comparison with pure PPC. However, its preparation process is very complicated.

MA is an inexpensive and easily accessible material. Simple preparative procedures such as melt compounding[23] and solution-based methods[11] have been used to end-cap PPC with MA. These studies found improvements in thermal stability compared to pure PPC, but no mechanical data was reported. In Lai et al.'s work,[24] it is demonstrated that end-capping PPC with maleic anhydride (MA) can result in an improvement in its thermal stability and mechanical properties, but it was not systematic studies regarding the end-capping effect of PPC. In this work, PPC is end-capped with MA via a simple melt blending process and the effect of MA content (from 0.5 to 5 wt %) on the thermal and mechanical properties of PPC will be investigated.

EXPERIMENTAL

Materials

Poly (propylene carbonate) (PPC) is obtained from State Key Polymer Physics and Chemistry Laboratory, Changchun Institute of Applied Chemistry, China. Its molecular weight measured by GPC is 2.48×10^5 g mol^{-1} and $M_w/M_n = 3.2$. Maleic anhydride (MA, >99.5%) was purchased from Tianjin Bodi Chemical (Tianjin, China).

End-capping PPC

PPC and MA (with the ratio of 100/0,100/0.5, 100/1,100/2,100/3,100/5) were melt mixed using a Hake Rheomix internal mixer at a barrel temperature of 130°C and a rotation speed of 50 rpm for 7 min. Prior to melt blending, PPC was dried in vacuum oven at 45°C for 5 h. Pure PPC was also processed in the internal mixer under the same condition to be used as reference. It is labeled as PPCMM. However due to the degradation of PPC during mixing, a large void content was observed in the pressed film. Therefore, the reference used for mechanical test in current study is hot pressed film from as received PPC powders. It is labeled as PPCM0. The final PPC/MA compounds (with MA content of 0.5, 1, 2, 3, and 5 wt %) were labeled as PPCM0.5, PPCM1, PPCM2, PPCM3, and PPCM5, respectively.

Characterizations

Fourier transform infrared (FT-IR) spectroscopy (FTIR)

FT-IR spectra with a resolution of 2 cm^{-1} and an average of 64 scans were recorded on Nicolet 560 IR Spectrum Scanner. All the samples were dissolved in chloroform at a concentration of 5w/v% and precipitated by ethanol. The dissolution/precipitation procedure was repeated to remove the ungrafted MA. The purified samples were dried under blast oven at 50°C for 12 h. The films tested by FT-IR were prepared by directly casting 1 wt % chloroform solutions onto KBr pellets and evaporating the solvent slowly.

Titration test

The grafting degree (G) of PPC-MA was defined as weight percent of grafted MA in PPC and determined from the titration of the purified PPC-MA, similar to that of the purified maleated poly(propylene carbonate) in Zhang et al.'s work.[23] PPC-MA was dissolved in chloroform at a concentration of 4 w/v% and precipitated by ethanol. The process is used to remove ungrafted MA. The purified PPC-MA was dried under vacuum at 50°C for 24 h. About 0.5 g of the well-dried PPC-MA was dissolved in 50 mL chloroform. The solution was titrated with 0.0132 potassium hydroxide solution in ethanol which was standardized by potassium hydrogen phthalate using phenolphthalein as the indicator. A blank test for PPC was carried out by the same method. G was calculated from the following equation:

$$G\,(\mathrm{wt}\,\%) = \frac{\frac{V_1 - V_0}{1000} \cdot N \cdot M_{MA}}{2W} \times 100\% = \frac{(V_1 - V_0)NM_{MA}}{2000W} \times 100\%$$

where, V_1 (mL) is base volume used for PPC-MA, V_0 (mL) is the base volume used for neat PPC, N (mol L^{-1}) the base concentration, W (g) the weight of sample and M_{MA} (g mol^{-1}) the molecular weight of MA.

Gel permeation chromatography (GPC)

The molecular weight (MW) and molecular weight distribution (MWD) of PPC was measured by gel permeation chromatography system (GPC, Agilent1100) with tetrahydrofuran (THF) as solvent. Calibration was performed with polystyrene standards.

Thermogravimetric analysis (TGA)

The thermal stability of pure PPC and PPC/MA blends were measured by thermogravimetric analysis

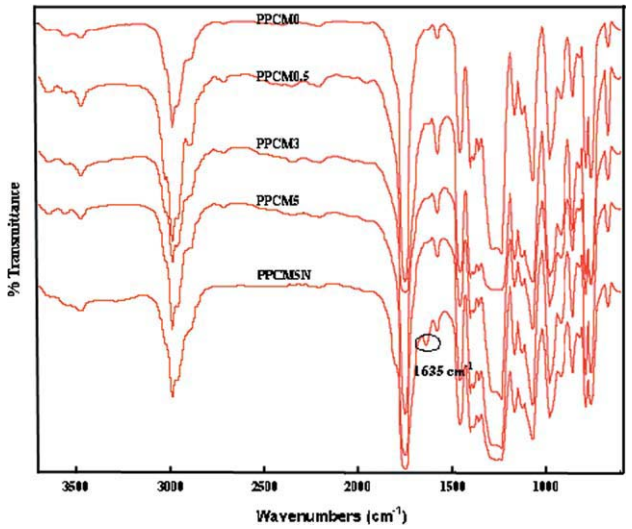

Figure 1 The FT-IR spectra of PPC and PPCM0.5, PPCM1, PPCM3, and PPCM5 in the range of 700–3300 cm^{-1}. [Color figure can be viewed in the online issue, which is available at wileyonlinelibrary.com.]

(TGA, WRT-2P, Shanghai Scale Factory). TGA test was performed from room temperature to 500°C at a heating rate of 15°C min^{-1} in nitrogen environment. The weight of the samples varied from 5 to 8 mg.

Mechanical testing

Tensile properties were tested by Universal Testing Machine in tension mode. Specimens used for tensile test were cut from the hot pressed films of PPC or PPC/MA. Those films were pressed at 130°C for 6 min. And the sample dimension was 4 mm in width, 0.4–0.5 mm in thickness, and 75 mm in length. Five samples were used for each measurement and averaged results are reported. The crosshead speed used was 10 mm min^{-1}.

Dynamic mechanical analysis (DMA)

Dynamic mechanical properties of the prepared composites (storage modulus and tan δ) were characterized by dynamic mechanical analyzer (DMA, Q800, TA Company) in tension mode. Temperature scan was conducted from −20 to 80°C at a heating rate of 3°C min^{-1}. A fixed frequency of 1 Hz was used. A static force of 0.01*N* and the force track of 120.0% were employed. The membrane was cut into the strip of 35 × 4 mm^2 for DMA test.

RESULTS AND DISCUSSION

Analysis of FTIR

To examine the possible interaction between PPC and MA, FTIR analysis was carried out and the results are shown in Figure 1. It should be noted that the dissociative MA which was not involved in the chemical reactions with PPC has been removed with ethanol solvent before the FTIR experiment. When FTIR spectra of PPCM5N (the sample containing unreacted MA which was not extracted) and PPCM5 (the extracted sample) are compared in Figure 1, the peak at 1635 cm^{-1} corresponds to (C=C) stretching which derives from MA[25] is seen to decrease upon purification.

This indicates that the extra MA exists as monomer when high content of MA is added. After purification, the FTIR spectrum of PPCM0.5, PPCM3, and PPCM5 are almost the same as PPC. However, it is known from literature that MA can be grafted onto PPC molecules by reactive blending.[23] The scheme is shown as Scheme 1.[23]

The cyclic anhydride group in MA exhibit an intensive absorption band near 1780 cm^{-1} and a weak band near 1850 cm^{-1}, due to the symmetric and asymmetric stretching of C=O, respectively.[26,27] However, it is noted from the FTIR spectra at these positions that there is no obvious difference between the spectra of neat PPC(labeled as PPCM0) and PPCM5N (which contains MA monomer). The reason behind this might be that the C=O stretch peak in pure PPC is broad and overlaps the stretching adsorption peak of C=O in MA. The cyclic anhydride group was opened after graft reaction. Therefore, the adsorption peak of C=O in anhydride group is shifted to the range between 1750 and 1715 cm^{-1}. It is very difficult to observe the difference after graft reaction as the content of MA on PPC chains is very low. A similar result has been reported by Lai et al.[28] As a dramatic increase in mechanical and thermal properties has been obtained in our study (see Figs. 3 and 6), it is thought that graft reactions have occurred in the process, further investigation will be carried out in the following study to demonstrate the graft of MA onto PPC. Furthermore, carboxyl group can be obtained in the graft reaction, but there is no obvious absorption peak of hydroxyl group in the FTIR spectra (above 3000 cm^{-1} [25]). There are two possible reasons for this: the graft amount is small; macromolecular coupling or crosslinking reaction

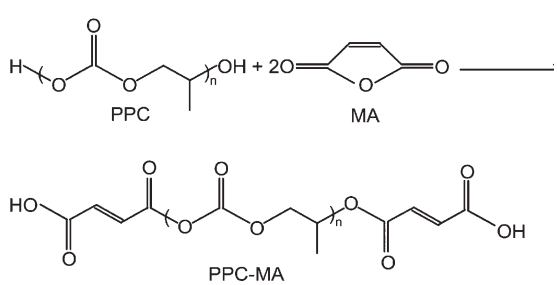

Scheme 1 Melt end-capping PPC with MA.

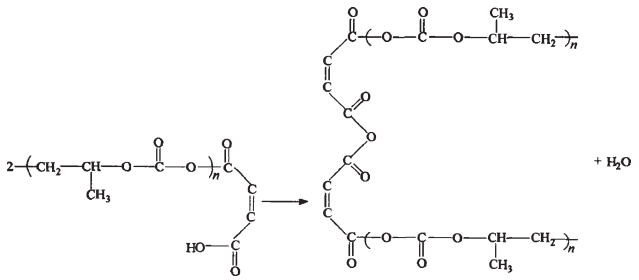

Scheme 2 Schematic representation of the macromolecular coupling or cross-linking reaction of MAPPC.

which takes place between the end carboxyl groups of MA-PPC during melt process as reported by Lai et al.[28] The scheme is shown in Scheme 2.[28]

This process consumes carboxyl groups and increases the molecular weight of polymer matrix. This might be responsible for the increase in strength observed in tensile test. The C=C stretching adsorption peak of PPC blends is as weak as pure PPC, the reason may be the low MA content grafted on PPC.

Titration test

To characterize the grafting degree (*G*) of MA on PPC, a titration test was carried out. Figure 2 shows the grafting degree of MA on the PPC with various MA content during reactive blending. It is shown that the content of MA grafted on PPC is quite low, which might be caused by an insufficient melt mixing condition used during reactive blending. Therefore, the active reactive sites are few, which directly resulted in low MA grafting degree.

There are three possible reactions taking place during reactive blending of MA and PPC. The reactions are MA end-capping PPC, MA grafting onto PPC backbone during free-radical reaction and

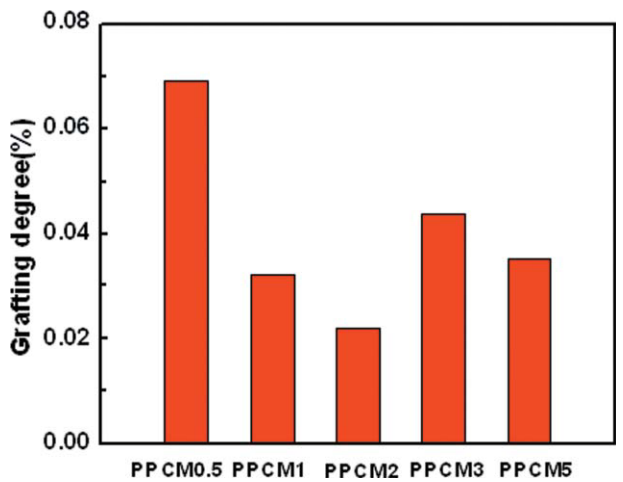

Figure 2 Grafting degree of end-capped PPC with different MA content. [Color figure can be viewed in the online issue, which is available at wileyonlinelibrary.com.]

TABLE I
The Weight Average Molecular Weight (MW), Molecular Weight Distribution (MWD) of Pure and End-Capped PPC

	MW	MWD
PPCM0	2.4804e5	3.2022e0
PPCMM	1.6039e5	4.3973e0
PPCM0.5	2.3660e5	2.6539e0
PPCM1	2.1383e5	2.7602e0
PPCM2	2.2100e5	2.9467e0
PPCM3	2.1104e5	3.2049e0
PPCM5	1.8823e5	2.6808e0

macromolecular coupling or crossing-linking of MA-PPC as shown in Scheme 2. The coupling reaction would lead to an increase in the molecular weight (see Table I).

GPC measurement

To understand the effect of processing on the molecular weight of PPC, the materials were further studied by GPC measurements. The weight average molecular weight (MW) and the molecular weight distribution (MWD) of PPC and PPC/MA blends are summarized in Table I. One can clearly see that the molecular weight of pure PPC drop sharply and MWD increased obviously after internal mixing. This was due to the thermal decomposition of PPC molecular chain under the processing conditions used. However, MW was significantly increased and MWD was remarkably decreased by the addition of 0.5 wt % MA which indicates that MA serves as an end-capping agent. With the content of MA increasing, the Mw obviously decrease and MWD gradually increase. The mechanism might be that the end capping reaction is well performed for PPC at very low MA content (0.5 wt %), which lead to higher molecular weight due to the branching reaction shown in Scheme 2. The further increase of MA content may have hindered the reaction. As with increasing MA content, the chance for homopolymerization of MA increases, it competes with end-capping reaction and lead to a decrease in grafting degree. These results are consistent with the results from titration test.

Thermal stability

TGA and DTG are used to investigate the effect of MA on the thermal stability of PPC. Figure 3 shows the TGA and DTG curves of pure PPC (labeled as PPCM0) and PPC/MA blends. It can be clearly observed from Figure 3(a) that the thermal degradation temperature was significantly improved with the addition of MA. In TGA test, three parameters were measured: the thermal degradation temperature at 5% weight loss ($T_{d,5\%}$), the temperature at

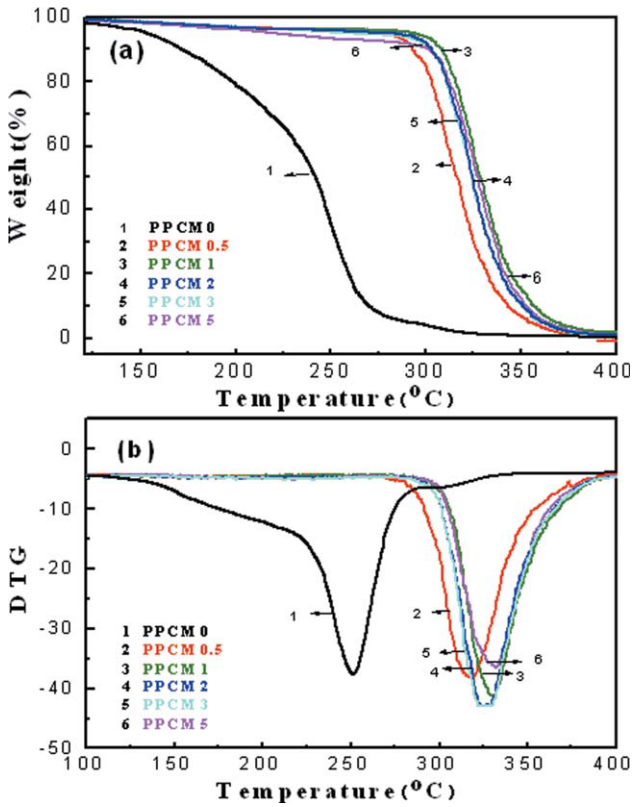

Figure 3 Thermogravimetric curves including (a) weight loss and (b) derivative thermometric curve for pure and end-capped PPC at a heating rate of 15°C min^{-1} in nitrogen gas. [Color figure can be viewed in the online issue, which is available at wileyonlinelibrary.com.]

50% weight loss ($T_{d,50\%}$), and the temperature at maximum weight loss ($T_{d,max}$). The summary of TGA results is listed in Table II. The $T_{d,5\%}$ of PPCM0 is obviously improved by the addition of MA and the maximum $T_{d,5\%}$ (occurring at PPCM1) reaches 292°C, it is 140°C higher than that of PPCM0. However, $T_{d,50\%}$ shows a decrease with further increasing MA content. $T_{d,50\%}$ also shows a remarkable increase by the presence of MA. For example, $T_{d,50\%}$ increases from 242 to 329°C with the addition of 1 wt % of MA in neat PPC. A similar trend is observed for $T_{d,max}$. These results indicate the successful end-capping of PPC.[11] Much better thermal stability is achieved compared with pure PPC. The decreased thermal stability for high MA content (PPCM3, PPCM5) has confirmed the results discussed in above section. It is mainly caused by the decreased end-capping efficiency at higher MA loadings.

In terms of the decomposition mechanism, Inoue et al.[29] reported that both chain unzipping and random chain scission operate during the decomposition of PPC chains with random chain scission occurs at higher temperatures compared with chain unzipping. Such a mechanism was further demonstrated by Peng et al.[11] Figure 3(b) illustrates the DTG curves of both pure PPC and PPC/MA blends. One can see that the peak temperature of the end-capped PPC shifts to a much higher temperature compared to PPCM0. It is also interesting to find that the DTG curve of PPCM0 is different from end-capped PPC. For PPCM0, the DTG curve shows two peaks. One occurs at about 200°C, which is characteristic of chain unzipping. And the other occurs at about 250°C, which corresponds to the mechanism of random chain scission. However, the DTG curve of all the end-capped PPC has only one peak, which indicates that initial chain unzipping from the terminal group is inhibited by end-capped PPC. These results agree well with the results reported by Peng et al.[11]

Kinetics of thermal degradation

Many methods have been used to calculate the kinetic parameters of thermal degradation by TGA measurements. Chang's method[30] is the most commonly used one. It is based on the following equation: $\ln(d\alpha/dt) - n\ln(1-\alpha) = \ln A - E/RT$. In this equation, A, E, and R represents the pre-exponential factor, the activation energy (J mol^{-1}) and the universal gas constant (8.314 J mol^{-1} K^{-1}), respectively; while α, t, T, and n are the conversion (weight of polymer volatilized/initial weight of polymer), the time (min) of reaction, the absolute temperature of reaction (K), and order of the thermal reaction, respectively. By plotting the left term of this equation versus $1/T$, a linear Region II part in the curves could be obtained if a suitable n value is selected (see Fig. 4). And the E and $\ln A$ values can be obtained from the slope and intercept of the straight line, respectively.

This method is used to calculate the kinetic parameters of pure PPC and end-capped PPC and the results are listed in Tables III and IV, respectively. Figure 4 shows plots of $\ln(d\alpha/dt) - n\ln(1-\alpha)$ against $1/T$ for pure PPC. Different degradation order (2, 2.5, 3, and 3.5) is used and a suitable n value of 3.5 is chosen because when selected this n value a linear Region II part in the curves could be obtained. The conversion ranges are from 5 to 90%. It can be seen that all curves can be divided into three parts: two linear parts and one transition

TABLE II
Thermal Gravimetric Parameters of Pure and End-Capped PPC

	$T_{d,5\%}$ (°C)	$T_{d,50\%}$ (°C)	$T_{d,max}$ (°C)
PPCM0	152	242	252
PPCM0.5	276	317	318
PPCM1	292	329	330
PPCM2	272	325	327
PPCM3	252	325	326
PPCM5	216	328	331

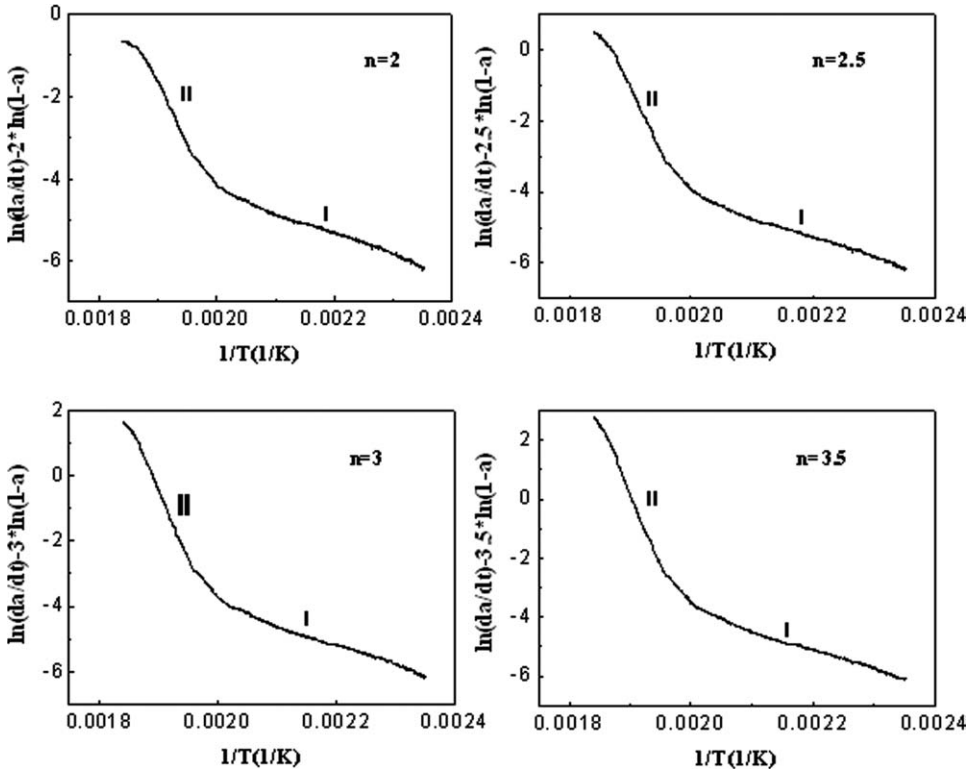

Figure 4 Plots of $\ln(d\alpha/dt) - n\ln(1 - \alpha)$ versus $1/T$ for pure PPC.

part. It is shown in the curves that the slopes of two linear parts are different. This is related to the activation energy (E), which indicates that during the degradation of pure PPC there are different dominant mechanisms.[13] These three parts correspond to chain unzipping from the terminal group (Region I), competing multi-step reactions (transition region) and random chain scission (Region II), respectively. This observation is consistent with the result from TGA curves for pure PPC.

Figure 5 shows plots of $\ln(d\alpha/dt) - n\ln(1 - \alpha)$ against $1/T$ for end-capped PPC with different MA content. It can be seen from Figure 5(a,b) that good linear relationship is obtained only for PPCM0.5 and PPCM1. The kinetic parameters of PPCM0.5 and PPCM1 can be seen in Table IV. The values for activation energies are 357.6 and 395.3 kJ mol^{-1}, respectively, equivalent to E_2 for pure PPC when n value is 3.5 (see Table III). This suggests that the main mechanism of degradation for PPCM0.5 and PPCM1 is random chain scission, which is the same as that of pure PPC in Region II. This could due to the good end-capping effect of low content of MA, which effectively prevents the chain unzipping of PPC. However, for PPCM2, PPCM3, and PPCM5, through selecting suitable n value one can observe a flat region is accompanied by a linear part, the curves only show good linear relations for $1/T$ range from 0.0016 to 0.0018 as shown in Figure 5(c–e), respectively. This flat region corresponds to the first region of pure PPC, which indicates that chain unzipping still happens in these samples. It is noted that the flat region becomes longer with increasing MA content. These results suggest that the thermal decomposition stability becomes worse with increasing MA content. As shown in the results obtained from GPC and FTIR measurement, the end capping effect is high enough for PPC at relatively low MA content. Further increase of MA content may have negative effect on end capping.

TABLE III
Kinetic Parameters for Pure PPC

Content of MA (%)	n	lnA	E (kJ mol^{-1})
0.5	3	70.2	357.6
1	3.3	76.3	395.3
2	2.7	68.6	355.2
3	2.5	64.0	333.3
5	2.3	56.0	298.2

TABLE IV
Kinetic Parameters for End-Capped PPC with Different MA Content

Value of n	E_1 (kJ mol^{-1})	$(\ln A)_1$	E_2 (kJ mol^{-1})	$(\ln A)_2$
2	204.6	45.0	43.8	6.3
2.5	270.1	60.6	48.3	7.5
3	335.7	76.2	52.7	8.8
3.5	401.2	91.9	57.2	10.0

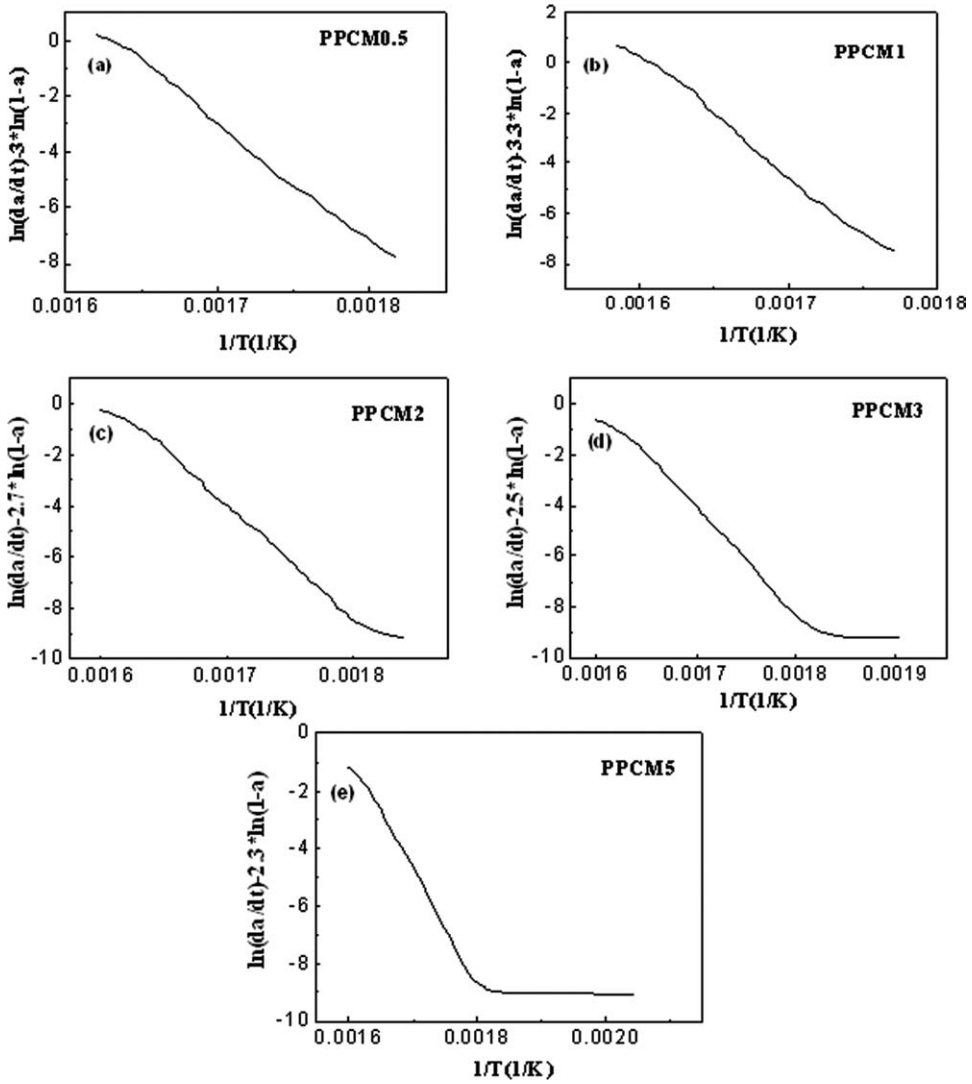

Figure 5 Plots of $\ln(d\alpha/dt) - n\ln(1-\alpha)$ versus $1/T$ for end-capped PPC with different MA contents.

Mechanical properties

Typical stress–strain curves of pure and end-capped PPC are shown in Figure 6 and the average values of tensile strength and elongation at break of various samples are shown in Figure 7. It is very interesting to see that the tensile strength is enhanced at lower MA content [see Fig. 7(a)]. The tensile strength increased from 3 to 27 MPa with the addition of 0.5 MA in PPC. It shows the interface between PPC polymer chains is effectively enhanced by end-capping MA onto PPC. Furthermore, the increased molecular weight (as shown in Table I) could also be partially responsible for this significant increase in tensile strength. More importantly, it has reached the strength of bulk polymers, such as PE[31] and PP.[32] It indicates the possibility to replace PE or PP with end-capped PPC. As PPC is synthesized from carbon dioxide, largely using PPC would enhance the effort to fight against well known global warming

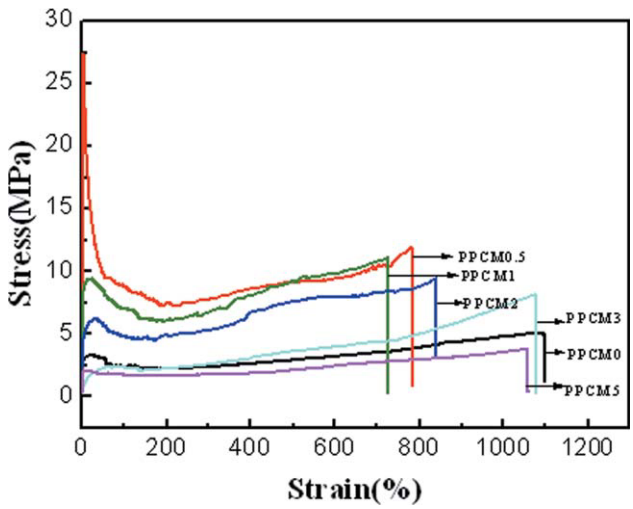

Figure 6 Stress–strain curves for pure and end-capped PPC. [Color figure can be viewed in the online issue, which is available at wileyonlinelibrary.com.]

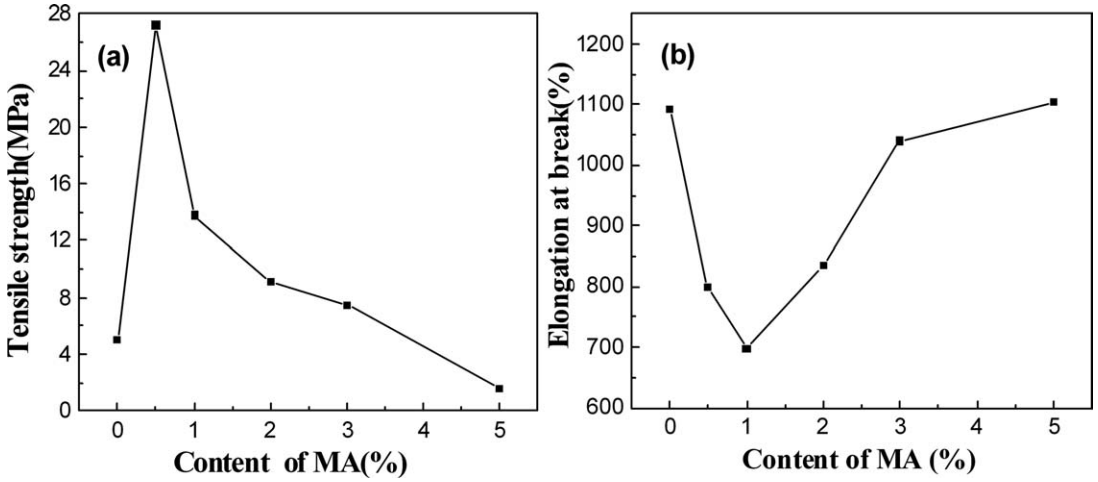

Figure 7 Variations of (a) tensile strength and (b) elongation at break for pure and end-capped PPC with different MA contents.

problem. Nevertheless, the tensile strength shows an obvious decrease with increasing MA content. For PPCM3 and PPCM5, the tensile strength decrease to the same level as pure PPC. From Figure 7(b), it can be observed that the elongation at break is decreased from 1100 to 800% and then 700% while 0.5 and 1 wt % is added into neat PPC, respectively. And then it increases with further increase of MA content and finally reaches the same level of pure PPC. From the GPC results, it is shown that the highest M_w and narrowest MWD are obtained for PPCM0.5. Furthermore, the highest grafting degree is obtained for PPCM0.5 (see Fig. 2). As a consequence, the highest tensile strength is observed for PPCM0.5. With increasing MA content, M_w slightly decrease and MWD gradually increase. This might be partially responsible for the trend in mechanical properties observed. Especially for PPCM3 and PPCM5, the homopolymerization of MA may dominate the reaction, and a decrease in the end capping efficiency is observed. These issues lead to a significant decrease in $T_{d,5\%}$ (see Table II) and tensile strength.

Dynamic mechanical properties

The enhancement of mechanical properties can be further demonstrated by the measurement of dynamic mechanical properties. The storage modulus and tan δ of pure and end-capped PPC as a function of temperature are shown in Figure 8. It is shown in Figure 8(a) that the storage modulus of PPCM0 is dramatically enhanced by the addition of 0.5–3 wt % MA in all the temperature range investigated. With the further increase of MA content, the storage modulus gradually decreased, especially at a high level of MA (PPCM5). It indicates that the stiffness of PPC/MA blends is improved by the addition

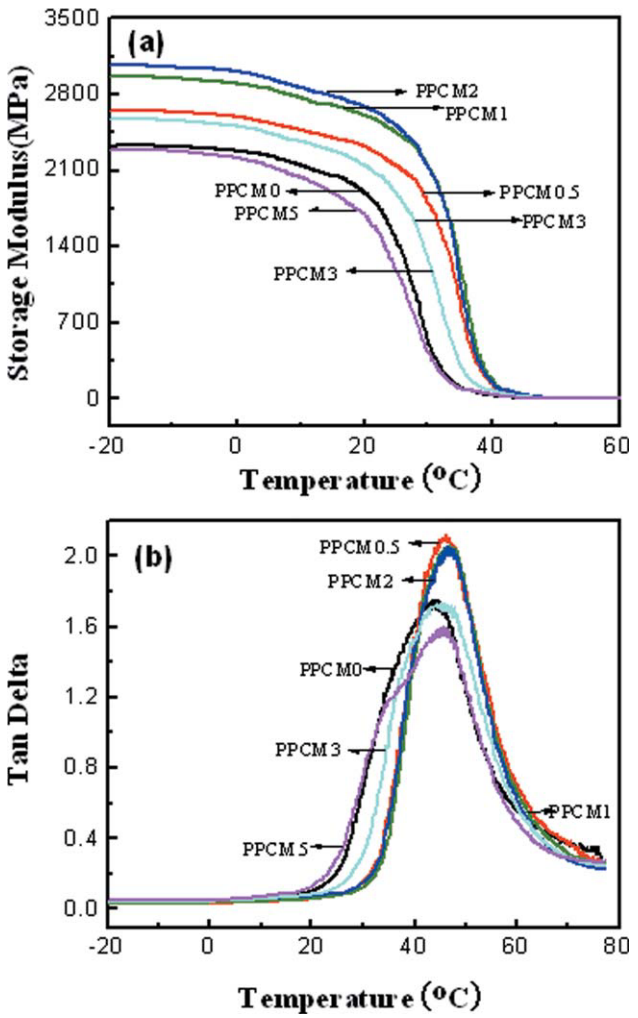

Figure 8 DMA curves including (a) storage modulus and (b) tan δ as a function of temperature for pure and end-capped PPC with different MA contents. [Color figure can be viewed in the online issue, which is available at wileyonlinelibrary.com.]

of small amount of MA. This result agrees well with the above mechanical property result. However, it can be noted that the storage modulus of all the systems decrease dramatically with increasing temperature. And they almost lost all their properties at 40°C. This is due to the amorphous nature of PPC, and it limits the application of PPC to low temperature applications or additives for other systems, such as PPC/PCL, PPC/PLA, etc.

Figure 8(b) presents the tan δ of pure PPC and PPC/MA blends versus temperature. The peak temperature corresponding to the glass transition temperature (T_g) of the sample. The T_g for PPCM0, PPCM0.5, PPCM1, PPCM2, PPCM3, and PPCM5 are 43.7, 46.2, 46.3, 46.6, 44.9, 45.4, respectively. It can be noted that the T_g of PPC is increased with the addition of MA. Furthermore, at small amount of MA contents (such as PPCM0.5, PPCM1, and PPCM2), the T_g is higher than that of PPCM3 and PPCM5. This result might due to the fact that the M_w of end-capped PPC is much higher and MWD is smaller than pure PPC. Therefore, the molecular chain mobility of end-capped PPC is much lower than pure PPC.

CONCLUSIONS

To improve the thermal stability and mechanical properties of a carbon dioxide sourced, environmental friendly polymer: PPC, efforts have been made to endcap MA onto PPC polymer chains. It is revealed that the addition of low content of MA during reactive blending showed good end-capping efficiency on PPC. The further increase of MA may hinder the reaction of MA with PPC, thus decreasing the end-capping efficiency. The thermal degradation temperature at 5% weight loss is improved by around 140°C by adding 1 wt % MA into pure PPC. The M_w was significantly enhanced and MWD was remarkably decreased with the addition of 0.5 wt % MA. This indicates the processability of PPC is significantly improved by grafting with small amount of MA. Furthermore, the tensile strength of PPC/MA blends with 0.5 wt % MA is nine times higher than pure PPC, which has approached the strength of bulk polymers, such as PP[31] and PE.[32] Nevertheless, it is shown in the DMA study that the storage modulus decreases sharply with increasing temperature. This limits the application of PPC to low temperature applications or additive for other blend systems.

References

1. Inoue, S.; Koinuma, H.; Tsurata, T. J Polym Sci Polym Lett Ed 1969, 7, 287.
2. Darensbourg, D. J.; Holtcamp, M. W. Macromolecules 1995, 28, 7577.
3. Super, M. S.; Beckman, E. Trends J Polym Sci 1997, 5, 236.
4. Tan, C. S.; Hsu, T. J Macromol 1997, 30, 3147.
5. Xu, J.; Li, R. K. Y.; Meng, Y. Z.; Mai, Y.-W. Mater Res Bull 2006, 41, 244.
6. Ma, X. F.; Yu, J. G.; Wang, N. J Polym Sci B Polym Phys 2006, 44, 94.
7. Ma, X. F.; Yu, J. G.; Zhao, A. Compos Sci Technol 2006, 66, 2360.
8. Zhu, Q.; Meng, Y. Z.; Tjong, S. C.; Zhao, X. S.; Chen, Y. L. Polym Int 2002, 51, 1079.
9. Lu, X. L.; Zhu, Q.; Meng, Y. Z Polym Degrad Stabil 2005, 89, 282.
10. Dixon, D. D.; Ford, M. E.; Montell, G. J. J Polym Sci Part C Polym Lett 1980, 18, 131.
11. Peng, S. W.; An, Y. X.; Chen, C.; Fei, B.; Zhuang, Y. G.; Dong, L. S. Polym Degrad Stabil 2003, 80, 141.
12. Li, X. H.; Meng, Y. Z.; Zhu, Q.; Tjong, S. C. Polym Degrad Stabil 2003, 81, 157.
13. Ge, X. C.; Li, X. H.; Zhu, Q.; Li, L.; Meng, Y. Z. Polym Eng Sci 2004, 44, 2134.
14. Zhang, Z. H.; Lee, J.-H.; Lee, S.-H.; Heo, S.-B.; Pittman, C. U. J Polym 2008, 49, 2947.
15. Yang, D. Z.; Hu, P. J Appl Polym Sci 2008, 109, 1635.
16. Shi, X. D.; Gan, Z. H. Eur Polym Mater 2007, 43, 4852.
17. Du, L. C.; Qu, B. J.; Meng, Y. Z.; Zhu, Q. Compos Sci Technol 2006, 66, 913.
18. Pang, H.; Liao, B.; Huang, Y. H.; Cong, G. M. J Appl Polym Sci 2002, 86, 2140.
19. Zhang, Z. H.; Zhang, H. L.; Zhang, Q. X.; Zhou, Q. H.; Zhang, H. F. J Appl Polym Sci 2006, 100, 584.
20. Mo, Z. S.; Zhao, X. J.; Wang, X. H. J Appl Polym Sci 2006, 100, 584.
21. Wang, N.; Zhang, X. X.; Yu, J. G.; Fang, J. M. Polym Int 2008, 57, 1027.
22. Tao, Y. H.; Wang, X.; Zhao, X. J.; Li, J.; Wang, F. S. J Polym Sci Part A Polym Chem 2006, 44, 5329.
23. Zhang, Z. H.; Shi, Q.; Peng, J.; Song, J. B.; Chen, Q. Y.; Yang, J. L.; Gong, Y. M.; Ji, R. H.; He, X. F.; Lee, J.-H. Polymer 2006, 47, 8548.
24. Lai, M. F.; Li, J; Liu, J. J. J Therm Anal Calorim 2005, 82, 293.
25. Liu, Y. X. Spectrum Analysis; Sichuan University Publishing Company, China, 2004.
26. Bellamy, L. J. The Infrared Spectra of Complex Molecules; Wiley: New York, 1964.
27. Pouchert, C. J. The Aldrich Library of infrared Spectra; Aldrich Chem Co: Milwaukee, WI, 1970.
28. Lai, M. F.; Li, J.; Yang, J.; Wang, J. F.; Liu, J. J Acta Polym Sin 2003, 6, 895.
29. Inoue, S.; Tsuruta, T.; Takada, T.; Migazaki, N.; Kambe, M.; Takaoka, T. Appl Polym Symp 1975, 26, 257.
30. Chang, W. L. J Appl Polym Sci 1994, 53, 1759.
31. Cheung, M. K.; Chan, D. Polym Int 1997, 43, 281.
32. Ning, N. Y.; Yin, Q. J.; Luo, F.; Zhang, Q.; Du, R. N.; Fu, Q. Polymer 2007, 48, 7374.